Available online at www.sciencedirect.com
ScienceDirect
Ceramics International 34 (2008) 1747–1751
CERAMICS INTERNATIONAL
www.elsevier.com/locate/ceramint

Biomimetic synthesis of spherical nano-hydroxyapatite in the presence of polyethylene glycol

Chaofan Qiu, Xiufeng Xiao, Rongfang Liu *

College of Chemistry and Materials Science, Fujian Normal University, Fuzhou 350007, PR China

Received 27 November 2006; received in revised form 1 April 2007; accepted 12 June 2007
Available online 9 August 2007

Abstract

Spherical nano-hydroxyapatite (nano-HA) was synthesized successfully by a biomimetic method using $Ca(NO_3)_2{\cdot}4H_2O$ and $(NH_4)_3PO_4{\cdot}3H_2O$ as reagents in the presence of polyethylene glycol (PEG). The crystalline phase, microstructure, chemical composition, and morphology of the obtained samples were characterized by X-ray powder diffraction (XRD), Fourier transform infrared spectroscopy (FTIR), and transmission electron microscopy (TEM). The results show that spherical nano-HA with diameter of 30–50 nm can be synthesized in the presence of a certain concentration (2–6%) of PEG. The crystallinity of HA powder synthesized in the presence of PEG was higher than that synthesized in the absence of PEG, but the crystallinity of HA reduced with increasing the concentration of PEG. The electrical conductivity (EC) of the solution revealed that PEG reduced the transfer rate of Ca^{2+} in the process of HA crystallization, indicating the interaction between PEG and HA. The possible mechanism of formation spherical nano-HA was discussed.

Keywords: Polyethylene glycol; Hydroxyapatite; Biomimetic; Spherical

1. Introduction

Hydroxyapatite (HA, chemical formula $Ca_{10}(PO_4)_6(OH)_2$) has received much attention in recent years [1,2]. HA is used as a bioceramic due to its bioactivity and osteoconductive properties in vivo [3,4]. The advantage of using HA as a bioceramic or biomaterial compared to other bioceramics, such as bioglass or A-W glass–ceramic, is its chemical similarity to the inorganic component of bone and tooth. It exhibits no cytoxic effects and shows excellent biocompatibility with hard tissues, skin and muscle tissues [5]. Due to these, HA has been applied clinically both as a dense, sintered material and as a coating on metallic implants [6,7]. In recent years, with the rapid development of the research of the nanometer HA material, the researchers also have a further understanding of the characteristic of HA, and have developed many new ways of using the nanometer HA, such as orthopedic, drug release, biomolecules separation, etc.

The shape of HA crystal can affect many characteristics of HA, such as surface characteristics, bioactivity and so on. Therefore, if we can control the crystal shape of the nanometer HA, such as needle-like, spherical, plate-like shape and so on, then we can expand the applications of the HA.

At present many studies have reported to synthesize the nanometer HA with different shapes. For example, the needle-like HA has been synthesized by different processing methods including organic gel systems, homogeneous precipitation or hydrothermal technology [8,9]; the rod-like HA has been synthesized by precipitating calcium nitrate tetrahydrate and ammonium dibase phosphate in the presence of polyacrylic acid followed by hydrothermal treatment [10]. However, the synthesis of the spherical nanometer HA by biomimetic method was rarely reported so far.

Polyethylene glycols (PEG) are polymers from oxyethylene polymerization, which are amphipathic and biocompatible polyethers widely used for biomedical research and applications [11]. On the other hand, PEG in aqueous solution are highly mobile molecules with large exclusion volume, and mainly free of charges which can avoid the strong interaction between the constituents [12]. A significant number of studies have reported that the presence of PEG can modify or control

* Corresponding author. Tel.: +86 591 83465190; fax: +86 591 87609532.
E-mail address: rfliu@vip.sina.com (R. Liu).

0272-8842/$34.00
doi:10.1016/j.ceramint.2007.06.001

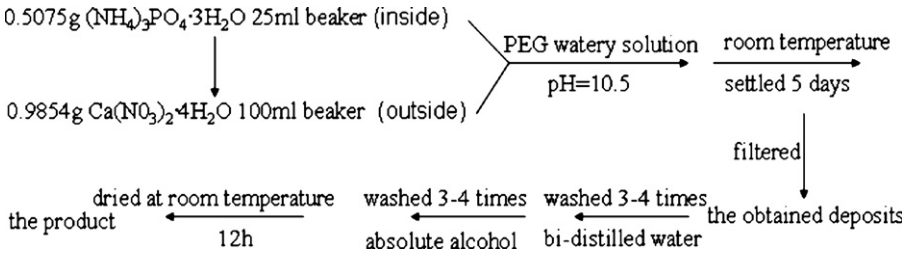

Fig. 1. Schematic illustration of the process followed for preparation of sample.

the surface of the nanometer crystal, moreover can act as the dispersing agent of the nanometer crystal in the process of synthesis [13–15].

This study takes $Ca(NO_3)_2{\cdot}4H_2O$ and $(NH_4)_3PO_4{\cdot}3H_2O$ as reagents to successfully synthesize the spherical nanometer HA in the presence of a certain concentration(2–6%) of PEG by biomimetic method, and it provides one new method to change the crystal habit of HA. At the same time the correlation of the crystal shape of the nanometer HA and the concentration of the PEG is also investigated. According to this correlation, the spherical nano-hydroxyapatite, whose size is about 30–50 nm, can be synthesized in the presence of a certain concentration of the PEG by biomimetic method.

2. Materials and experimental methods

2.1. Materials

Polyethylene glycol (MW6000), $(NH_4)_3PO_4{\cdot}3H_2O$ (AR), $Ca(NO_3)_2{\cdot}4H_2O$ (AR), absolute alcohol (AR) and ammonia solution (AR), which were purchased from Sinopharm Chemical Reagent Co. Ltd. (Shanhai, China) were used as the initial chemicals.

2.2. Preparation of the samples

First, 0.9854 g $Ca(NO_3)_2{\cdot}4H_2O$ was spread at the bottom of a 100 ml beaker; at the same time, 0.5075 g $(NH_4)_3PO_4{\cdot}3H_2O$ was spread at the bottom of a 25 ml beaker. The preparation of the sample is based on the following reaction equation with Ca/P molar ratio of 1.67, which was standard stoichiometry for pure HA [16]:

$$10Ca^{2+} + 6PO_4^{3-} + 2OH^- = Ca_{10}(PO_4)_6(OH)_2$$

Then, the 25 ml beaker was put inside the 100 ml beaker just above the bottom of the 100 ml beaker. The mass percent concentration of PEG watery solution is respectively 0.00, 0.01, 0.10, 1.00, 2.00, 3.00, 4.00, 5.00 and 6.00% (the pH of the PEG solution was adjusted to 10.5 by the addition of NH_3 solution), which was slowly dripped into the 25 ml beaker using the fixed isopiestic-pressure-funnel until the 25 ml beaker was full. Then, the PEG solution was dripped into the 100 ml beaker at the same way until the outside liquid level almost reached the inside liquid level. After the whole system was kept still for 5 min to let calcium ions react with PEG, PEG solution was dripped again until the liquid level was 5 mm higher than the height of the 25 ml beaker. The big beaker was sealed with the preservative film and settled for 5 days under room temperature. The obtained deposits were washed 3–4 times by bi-distilled water and the absolute alcohol, respectively. The obtained deposits were filtered, then dried at room temperature for 24 h. The schematic illustration of the process followed for preparation of samples is shown in Fig. 1.

2.3. Characterization of the samples

The morphologies of as-prepared samples were observed by Hitachi 600 Transmission Electron Microscopy (TEM). The surface composition and structure of as-prepared samples were determined by using X-ray powder diffraction (XRD) and Fourier transform infrared spectroscopy (FTIR). Phases identification was achieved by comparing the diffraction patterns of HA with ICDD (JCPDS) standards. Philips X'Pert MPD diffractometer with Cu Kα radiation was used, the X-ray generator was operated at 40 KV; and 40 mA. Date sets were collected within the range of 5–90° with a step size of 0.02° and a count rate of 3.0 °/min. FTIR spectra were obtained by using Nicolet Avatar 360 spectrometer. Spectra were obtained at 4 cm^{-1} resolution averaging 64 scans. The electrical conductivity was determined by the conductometer DDS-11A (Shanghai, China). The pH values of the PEG solution were measured using a digital pH meter (828, Orion).

3. Results

3.1. The crystal shape of the obtained products

Fig. 2a–h are the TEM micrographs of the samples which were synthesized using $Ca(NO_3)_2{\cdot}4H_2O$ and $(NH_4)_3PO_4{\cdot}3H_2O$ as reagents with or without PEG. Fig. 2a is the TEM micrograph of the sample which was synthesized in the absence of PEG, the granules agglomerate seriously, and the shape of the samples is mainly the shape of floccule. Fig. 2b and c are the TEM micrographs of the samples which were synthesized in the low concentration of PEG (lower than 1%), as shown in figure, most of the particles are spherical, some are small needle-like. Fig. 2d–g are the TEM micrographs which were synthesized in the high concentration of PEG. As shown in Fig. 2d–f, with increasing the concentration of PEG (2–4%), the shapes of particles are mainly spheroid, but the edge of the granules is not very smooth. When the concentration of PEG is high than 5%,

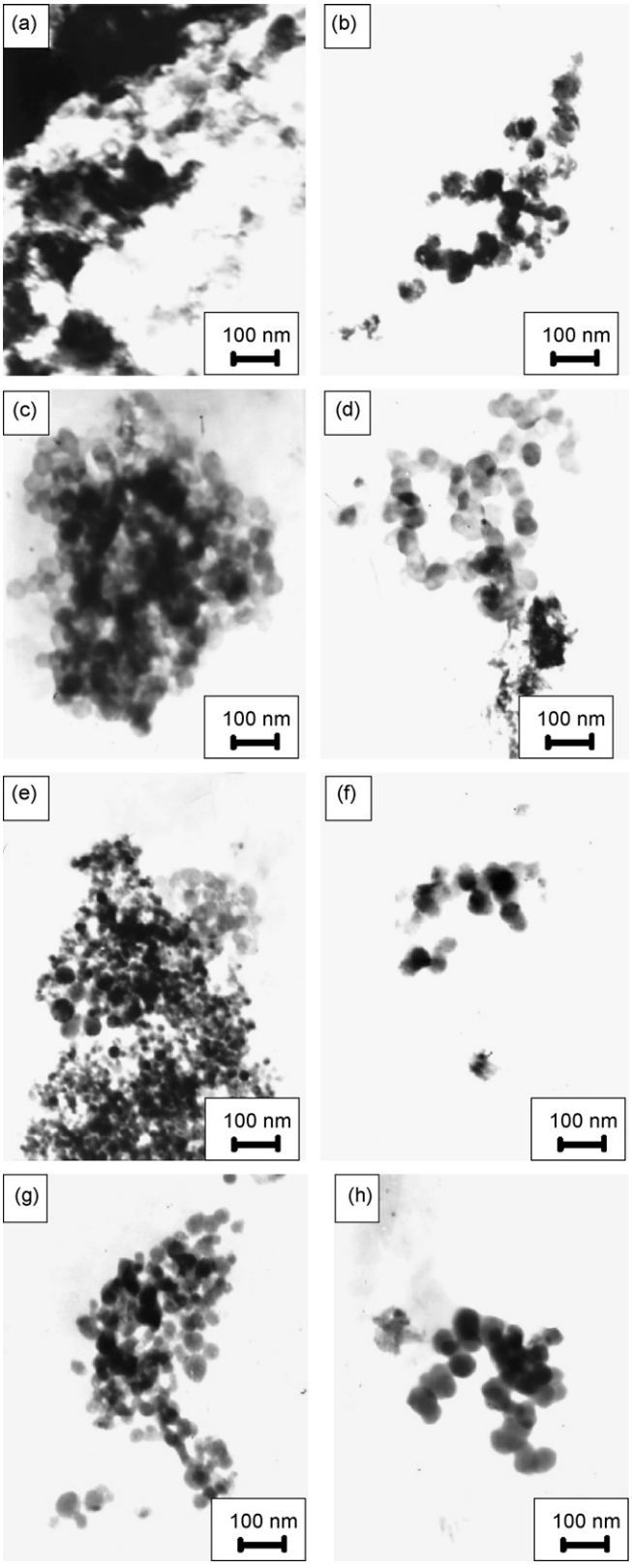

Fig. 2. TEM micrographs of samples: (a) the absent of PEG, PEG: (b) 0.1%, (c)1.0%, (d) 2.0%, (e) 3.0%, (f) 4.0%, (g) 5.0%, and (h) 6.0%.

Table 1
Electrical conductivity of $Ca(NO_3)_2$ and $Ca(NO_3)_2$–PEG solution

$c(Ca(NO_3)_2)$ (mol L^{-1})	0.01	0.02	0.03	0.04	0.05
$s_1(Ca(NO_3)_2)$ (ms cm^{-1})	1.80	3.12	4.15	5.25	6.05
$s_2(Ca(NO_3)_2$–PEG) (ms cm^{-1})	1.70	3.00	4.00	5.05	5.85
$\Delta s = s_1 - s_2$	0.10	0.12	0.15	0.20	0.20

as shown in Fig. 2g and h, the shapes of particles are smooth spherical, and the particles size probably are about 30–50 nm.

3.2. The electrical conductivity of the solution

In order to investigate the function of PEG during the nucleation and growth of HA, the electrical conductivity were measured under different concentration of $Ca(NO_3)_2$ solution and $Ca(NO_3)_2$–PEG (the mass percent concentration of PEG all are 1%) solution, the results lists in Table 1.

Table 1 lists the results of the conductivity measurement. Comparing with the electrical conductivity of the $Ca(NO_3)_2$ solution, the conductivity of the $Ca(NO_3)_2$–PEG solution decreases obviously, and the difference value of them($\Delta s = s_1 - s_{2)}$ increases from 0.10 to 0.20 ms cm^{-1} with increasing the concentration of Ca^{2+}, indicating the interaction between Ca^{2+} and PEG. This interaction reduced the transfer rate of Ca^{2+}, thus the electricity conductivity of the solution reduced. The interaction between Ca^{2+} and PEG, possibly is one of influence factors of the nucleation and growth of the spherical HA crystal.

3.3. XRD and FTIR of the as-prepared samples

XRD patterns of as-prepared samples in the presence of different concentration of PEG are shown in Fig. 3. As shown in Fig. 3, the characteristic peaks at $2\theta = 26.12$, 32.13 are

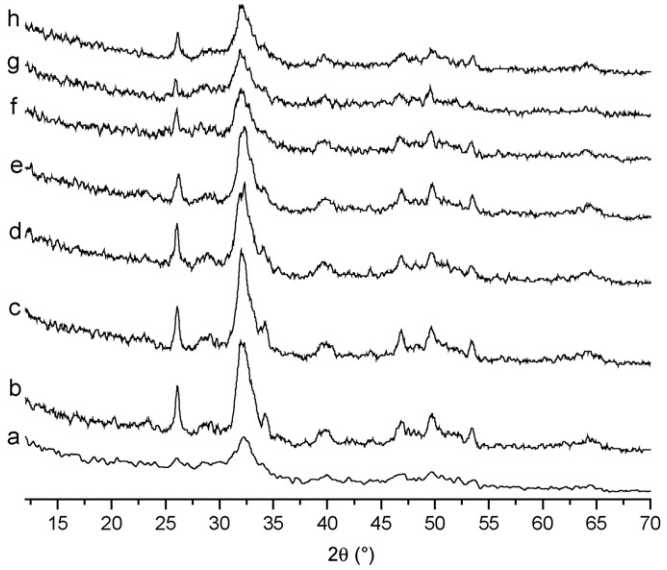

Fig. 3. XRD patterns of obtained samples in the presence of PEG with different concentration: (a) the absent of PEG, PEG: (b) 0.1%, (c)1.0%, (d) 2.0%, (e) 3.0%, (f) 4.0%, (g) 5.0%, and (h) 6.0%.

correspond to the standard diffraction card of HA (JCPDS 09-432) without other phases being detected. Fig. 3b–h shows the XRD pattern of the as-prepared samples synthesized in the presence of PEG. The results show that the diffraction peak of the samples synthesized in the presence of PEG are higher and narrower than that of prepared in the absence of PEG, indicating larger crystallites and higher crystallinity. However, these diffraction peaks become wider and less with increasing the concentration of PEG. The broadened peak observed in Fig. 3b–h indicate the presence of submicron crystallites in the powders. As the particle size is in the range of submicron to nano-meter, the peaks would be broadened.

FTIR spectra of the as-prepared samples in the presence of PEG with different concentration are shown in Fig. 4. The intense band at 1034 cm^{-1} corresponds to P–O stretching vibration modes of PO_4^{3-} groups, whereas the bands at 471, 561, and 604 cm^{-1} correspond to the O–P–O bending mode. The doublet at 1420 and 1460 cm^{-1} and 872 cm^{-1} is assigned to CO_3^{2-} groups. The broad band at 3437 cm^{-1}, as well as the band centered at 1624 cm^{-1}, correspond to H_2O adsorbed on the surface. As shown in Fig. 4, the adsorption bands of all groups does not change significantly with increasing the concentration of PEG, therefore, the effect of the concentration of PEG on the structure of HA can not be judged from FTIR spectra. However, all the spectra lack the characteristic absorption bands of hydroxyl group, this is probably due to a low degree of crystallinity.

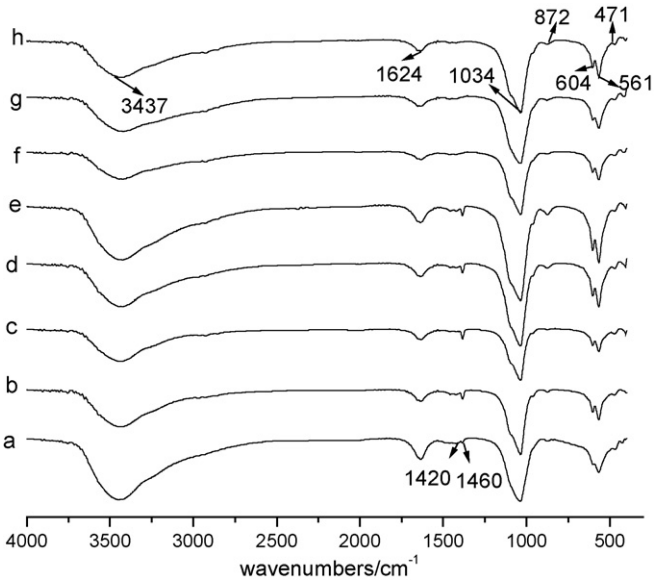

Fig. 4. FTIR spectra of obtained samples in the presence of PEG with different concentration: (a) the absent of PEG, PEG: (b) 0.1%, (c)1.0%, (d) 2.0%, (e) 3.0%, (f) 4.0%, (g) 5.0%, and (h) 6.0%.

4. Discussion

The stereochemistry structure of PEG in the absence of water or in the aqueous solution and the possible formation process of HA in the presence of PEG are shown in Fig. 5.

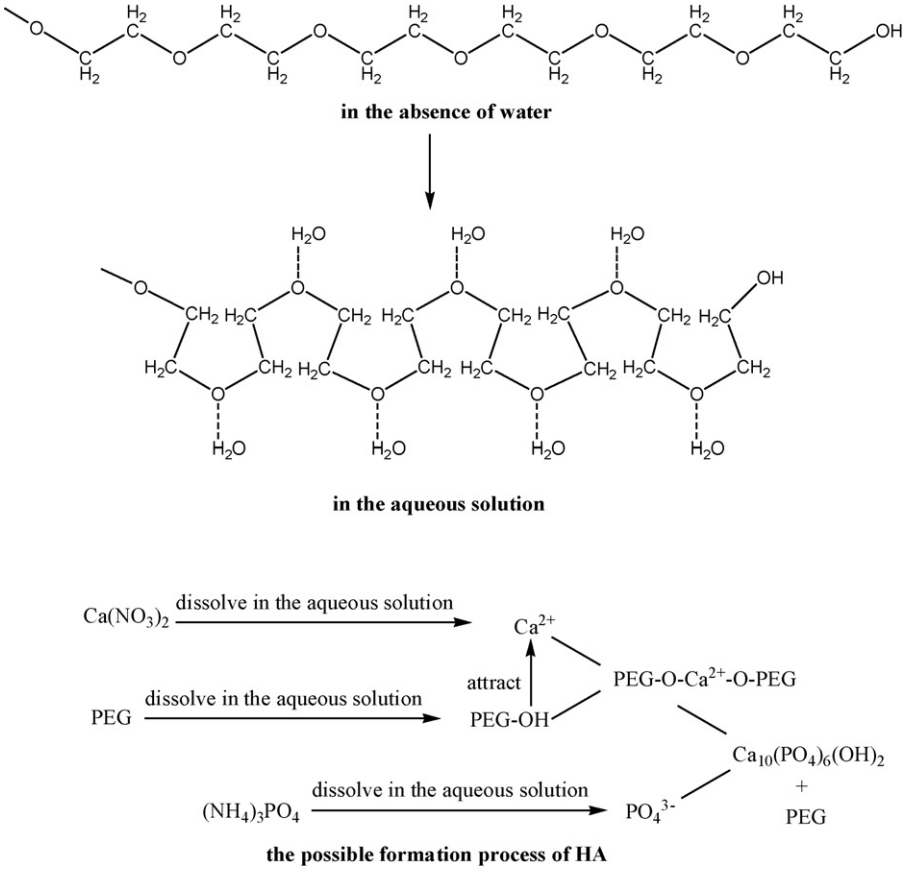

Fig. 5. The stereochemical structure of PEG and schematic illustration of the possible process of the forming of HA.

When PEG was dissolved in the aqueous solution, the PEG–OH bond was formed [17]. PEG molecule has the ability to chelate Ca^{2+}[18], therefore, PEG–OH can attract Ca^{2+} released from the $Ca(NO_3)_2{\cdot}4H_2O$ to form the bond of PEG–O–Ca^{2+}–O–PEG, then PEG–O–Ca^{2+}–O–PEG reacted with the PO_4^{3-} released from $(NH_4)_3PO_4{\cdot}3H_2O$ to produce HA crystal nucleus. In this process, the release rate of Ca^{2+} and PO_4^{3-} are the important factor. The electrical conductivity experiments show that the release rate of Ca^{2+} reduced with increasing the concentration of PEG (Table 1). Experiments show that a large amount of deposits form in a short time when the solution was in the absence of PEG or the concentration of PEG was quite low, indicating HA produced quickly. With increasing the concentration of PEG, initial deposits were gradually reduced and it required longer time to produce large quantities of deposits, indicating that PEG reduced the release rate of Ca^{2+} and restrained the formation of HA crystal nucleus. When the release rate of Ca^{2+} and the deposit rate of HA crystal nucleus deposited in the precipitation center achieved a dynamical equilibrium, HA crystal nucleus deposited isotropically, and finally the spherical HA particles were obtained. When the concentration of PEG was low, the release rate of Ca^{2+} were very fast and a large number of HA crystal nucleus were produced, HA crystal nucleus could not deposited isotropically in the precipitation center, so the morphology of as-prepared HA particles were not spherical.

As shown in Fig. 3, the crystallinity of HA reduced with increasing the concentration of PEG, indicating that PEG could possible cause distortion of the structure. The distortion structure and low crystallinity of HA crystal would increase the surface energy of HA crystal. Therefore, HA crystal inclined to form the spherical morphology to lower the surface energy. Obviously, as shown in Fig. 2 the more HA crystal prefer to form the spherical morphology with increasing the concentration of PEG. Therefore, the effect of the concentration of PEG on the morphology of HA crystal can be concluded in the following three aspects. Firstly, PEG modified or controlled the surface of the nanometer crystal. Secondly, PEG controlled the reaction speed of the reactant. Thirdly, PEG acted as the dispersing agent of the nanometer crystal.

5. Conclusions

Spherical nano-hydroxyapatite could be synthesized successfully by a biomimetic method using $Ca(NO_3)_2{\cdot}4H_2O$ and $(NH_4)_3PO_4{\cdot}3H_2O$ as reagents in the presence of PEG. The results indicated that the concentration of the PEG significantly affected the morphologies of the nanometer HA. Spherical HA crystallites with 30–50 nm diameter can be synthesized successfully in the presence of a certain concentration (2–6%) of PEG. The crystallinity of HA synthesized in the presence of PEG reduced continuously with increasing the concentration of PEG. The interaction between Ca^{2+} and PEG, possibly is an important factor of the nucleation and growth of the spherical HA crystal.

Acknowledgements

The authors would like to thanks National Nature Science Foundation of China (30600149), the science research foundation of ministry of Health & United Fujian Provincial Health and Education Project for Tackling the Key Research, PR China (WKJ 2005-2-008) and Fujian Development and Reform Commission of China (No. 2004[477]).

References

[1] M. Jarcho, Calcium phosphate ceramic as hard tissue prosthetics, Clin. Orthop. 15 (1981) 259–278.
[2] M. Jarcho, J.F. Kay, K.I. Gunmaer, R.H. Doremus, H.P. Drobeck, Tissue, cellular and subcellular events at a bone–ceramic hydroxylapatite interface, J. Bioeng. 1 (1997) 79–82.
[3] S.H. Maxian, J.P. Zawaddsky, M.G. Dunn, Effect of Ca/P coating resorption and surgical fit on the bone/implant interface, J. Biomed. Mater. Res. 28 (1994) 1311–1319.
[4] M. Jarcho, C.H. Bolen, M.B. Thomas, J. Bobich, J.F. Kay, J. Doremus, HA synthesis and characterisation in dense poly-crystalline form, J. Mater. Sci. 11 (1976) 2027–2035.
[5] Y.F. Hu, X.G. Miao, Comparison of hydroxyapatite ceramics and hydroxyapatite/borosilicate glass composites prepared by slip casting, Ceram. Int. 30 (2004) 1787–1791.
[6] M. Akao, H. Aoki, K. Kato, Mechanical properties of sintered hydroxyapatite for prosthetic applications, J. Mater. Sci. 16 (1981) 809–812.
[7] R.M. Pilliar, J.E. Davies, D.C. Smith, The bone–biomaterial interface for load-bearing implants, MRS Bull. 16 (1991) 55–61.
[8] V.L. Alexeev, E.A. Kelberg, G.A. Evmenenko, Improvement of the mechanical properties of chitosan films by the addition of poly(ethylene oxide), Polym. Eng. Sci. 40 (2000) 1211–1215.
[9] N. Clavaguera, J. Saurina, J. Lheritier, J. Masse, A. Chauvet, M.T. Mora, Eutectic mixtures for pharmaceutical applications: a thermodynamic and kinetic study, Thermochim. Acta 290 (1997) 173–180.
[10] S. Zhang, K.E. Gonsalves, Preparation and characterization of thermally stable nanohydroxyapatite, J. Mater. Sci. Mater. Med. 8 (1997) 25–28.
[11] D.A. Herold, K. Keil, D.E. Bruns, Oxidation of polyethylene glycols by alcohol dehydrogenase, Biochem. Pharmacol. 38 (1989) 73–76.
[12] Y. Fujishiro, H. Yabuki, K. Kawamura, T. Sato, A. Okuwaki, Preparation of needle-like hydroxyapatite by homogeneous precipitation under hydrothermal conditions, J. Chem. Technol. Biotechnol. 57 (1993) 349–353.
[13] M.A. Malmsten, K.B. Emoto, J.M. Van Alstine, Effect of chain density on inhibition of protein adsorption by poly(ethylene glycol) based coatings, J. Colloid Interf. Sci. 202 (1998) 507–517.
[14] S. Sharma, K.C. Popat, T.A. Desai, Controlling nonspecific pProtein interactions in silicon biomicrosystems with nanostructured poly(ethylene glycol) films, Langmuir 18 (2002) 8728–8731.
[15] J.X. Duan, X.T. Huang, E. Wang, PEG-assisted synthesis of ZnO nanotubes, Mater. Lett. 60 (2006) 1918–1921.
[16] X.L. Tang, X.F. Xiao, R.F. Liu, Structural characterization of silicon-substituted hydroxyapatite synthesized by a hydrothermal method, Mater. Lett. 59 (2005) 3486–3841.
[17] P.C. Si, X.F. Bian, H. Li, Y.X. Liu, Synthesis of ZnO nanowhiskers by a simple method, Mater. Lett. 57 (2003) 4079–4082.
[18] S.F.A. Hossaing, J.A. Hubbell, Molecular weight dependence of calcification of polyethylene glycol hydrogels, Biomaterials 15 (1994) 921–925.